

Weak Gravitational Lensing by Large-Scale Structure

Alexandre Refregier

Service d’Astrophysique, CEA/Saclay, 91191 Gif sur Yvette, France;
email: refregier@cea.fr

KEYWORDS: Cosmology, Dark Matter, Cosmic Shear, Structure Formation, Statistics

ABSTRACT: Weak gravitational lensing provides a unique method to map directly the distribution of dark matter in the universe and to measure cosmological parameters. This cosmic-shear technique is based on the measurement of the weak distortions that lensing induces in the shape of background galaxies as photons travel through large-scale structures. This technique is now widely used to measure the mass distribution of galaxy clusters and has recently been detected in random regions of the sky. In this review, we present the theory and observational status of cosmic shear. We describe the principles of weak lensing and the predictions for the shear statistics in favored cosmological models. Next, we review the current measurements of cosmic shear and show how they constrain cosmological parameters. We then describe the prospects offered by upcoming and future cosmic-shear surveys as well as the technical challenges that have to be met for the promises of cosmic shear to be fully realized.

1 INTRODUCTION

Gravitational lensing provides a unique method to directly map the distribution of dark matter in the universe. It relies on the measurement of the distortions that lensing induces in the images of background galaxies (for reviews, see Bartelmann & Schneider 1999, Bernardeau 1999, Kaiser 1999, Mellier 1999, Narayan & Bartelmann 1996, Schneider 1995, Wittman 2002). This method is now widely used to map the mass of clusters of galaxies (see Fort & Mellier 1994 for a review) and has been extended to the study of superclusters (Gray et al. 2002, Kaiser et al. 1998) and groups (Hoekstra et al. 2001). Recently, weak lensing was statistically detected for the first time in random patches of the sky (Brown et al. 2003; Bacon et al. 2002; Bacon, Refregier & Ellis 2000; Hamana et al. 2003; Hämmerle et al. 2002; Hoekstra et al. 2002a; Hoekstra, Yee & Gladders 2002a; Jarvis et al. 2002; Kaiser, Wilson & Luppino 2000; Maoli et al. 2001; Refregier, Rhodes, & Groth 2002; Rhodes, Refregier & Groth 2001; van Waerbeke et al. 2000; van Waerbeke et al. 2001a; van Waerbeke et al. 2002; Wittman et al. 2000). These cosmic shear surveys provide direct measurements of large-scale structure in the universe and, therefore, of the distribution of dark matter. Unlike other methods that probe the distribution of light, weak lensing measures the mass and can thus be directly compared to reliable theoretical models of structure formation. Cosmic shear can therefore be used to measure cosmological parameters in the context of these models, thereby opening wide prospects for cosmology (Bernardeau, van Waerbeke & Mellier 1997; Hu & Tegmark 1999; Jain & Seljak

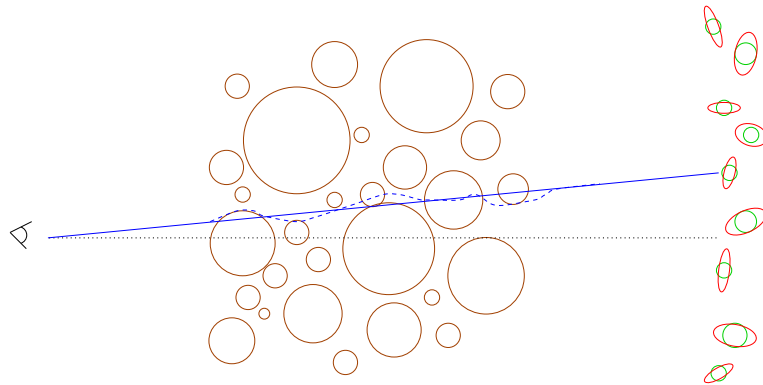


Figure 1: Illustration of the effect of weak lensing by large-scale structure. The photon trajectories from distant galaxies (*right*) to the observer (*left*) are deflected by intervening large-scale structure (*center*). This results in coherent distortions in the observed shapes of the galaxies. These distortions, or shears, are on the order of a few percent in amplitude and can be measured to yield a direct map of the distribution of mass in the universe.

1997; Kaiser 1998).

In the present review, we describe the theoretical and observational status of cosmic shear. Earlier reviews of this fast-evolving field can be found in Hoekstra et al. (2002b), Mellier et al. (2001), van Waerbeke et al. (2002), Wittman (2002). Here, we first describe the principles of weak lensing (Section 2). We then summarize the different statistics used to measure cosmic shear and describe how they are used to constrain cosmological parameters (Section 3). In Section 4, we survey the different methods used to derive the lensing shear from the shapes of background galaxies. We present, in Section 5, the current observations and their cosmological significance. Future cosmic-shear surveys and the prospects they offer for cosmology are described in Section 6. In Section 7, we outline how systematic effects present challenges that must be met for the potential of these future surveys to be fully realized. We summarize our conclusions in Section 8.

2 THEORY

The idea of cosmic shear can be traced back to a lecture given by Richard Feynman at Caltech in 1964 (J.E. Gunn, personal communication). Several theorists (e.g., Gunn 1967, Jaroszyński et al. 1990, Kristian & Sachs 1966, Lee & Paczyński 1990, Schneider & Weiss 1988) then studied the propagation of light in an inhomogeneous universe. Predictions for the statistics of the weak-lensing distortions were then computed in a modern cosmological context by several groups (Babul & Lee 1991, Blandford et al. 1991, Kaiser 1992, Miralda-Escudé 1991, Villumsen 1996). More recently, the power of cosmic shear to measure cosmological parameters was the object of many theoretical studies (Bernardeau, van Waerbeke & Mellier 1997; Jain & Seljak 1997; Hu & Tegmark 1999; Kaiser 1998; Kamionkowski et al. 1997; van Waerbeke, Bernardeau & Mellier 1999). In this section, we briefly describe the principles of weak lensing and show how this technique can be used to map the dark matter in the universe.

As they travel from a background galaxy to the observer, photons get deflected

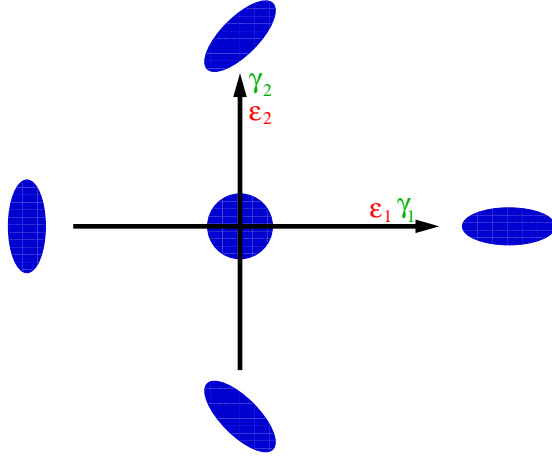


Figure 2: Illustration of the geometrical meaning of the shear γ_i and of the ellipticity ϵ_i . A positive (negative) shear component γ_1 corresponds to an elongation (compression) along the x -axis. A positive (negative) value of the shear component γ_2 corresponds to an elongation (compression) along the $x = y$ axis. The ellipticity of an object is defined to vanish if the object is circular (*center*). The ellipticity components ϵ_1 and ϵ_2 correspond to compression and elongations similar to those for the shear components.

by mass fluctuations along the line of sight (see Figure 1). As a result, the apparent images of background galaxies are subject to a distortion that is characterized by the distortion matrix:

$$\Psi_{ij} \equiv \frac{\partial(\delta\theta_i)}{\partial\theta_j} \equiv \begin{pmatrix} \kappa + \gamma_1 & \gamma_2 \\ \gamma_2 & \kappa - \gamma_1 \end{pmatrix}, \quad (1)$$

where $\delta\theta_i(\theta)$ is the deflection vector produced by lensing on the sky. The convergence κ is proportional to the projected mass along the line of sight and describes overall dilations and contractions. The shear γ_1 (γ_2) describes stretches and compressions along (at 45° from) the x -axis. Figure 2 illustrates the geometrical meaning of the two shear components.

The distortion matrix is directly related to the matter density fluctuations along the line of sight by

$$\Psi_{ij} = \int_0^{\chi_h} d\chi g(\chi) \partial_i \partial_j \Phi, \quad (2)$$

where Φ is the Newtonian potential, χ is the comoving distance, χ_h is the comoving distance to the horizon, and ∂_i is the comoving derivative perpendicular to the line of sight. The radial weight function $g(\chi)$ is given by

$$g(\chi) = 2 \int_\chi^{\chi_h} d\chi' n(\chi') \frac{r(\chi)r(\chi' - \chi)}{r(\chi')}, \quad (3)$$

where $r = a^{-1}D_A$, and D_A is the angular-diameter distance. The function $n(\chi)$ is the distribution of the galaxies as a function of the comoving distance χ from the observer and is assumed to be normalized as $\int d\chi n(\chi) = 1$.

As we discuss in Section 4, galaxy shapes can be averaged over a patch of the sky to measure the shear, which is thus an observable. The shear pattern expected in

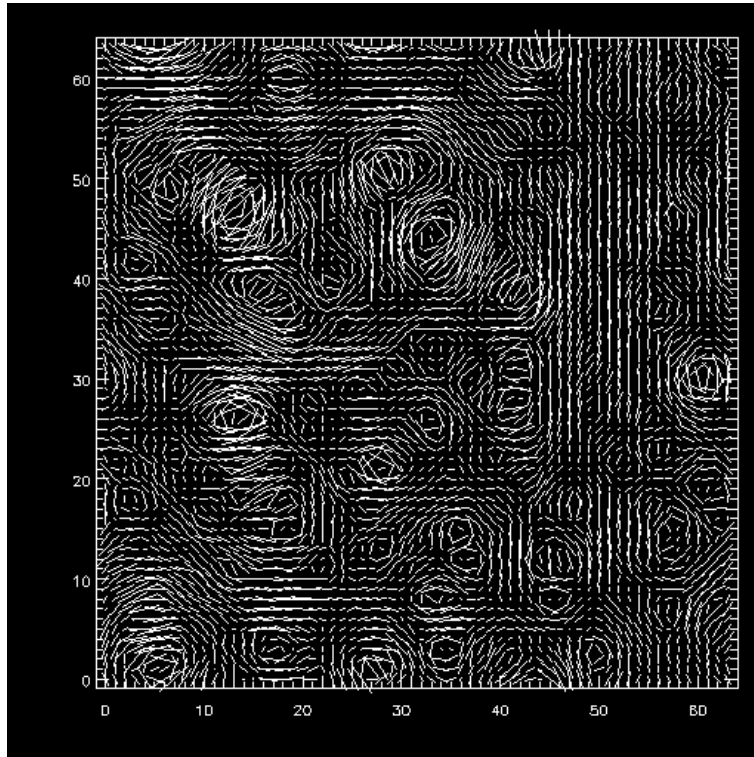


Figure 3: Shear map derived by ray-tracing simulations by Jain, Seljak & White (2000). The size and direction of each line gives the amplitude and position angle of the shear at this location on the sky. The displayed region is $1^\circ \times 1^\circ$ for an SCDM (Einstein-De Sitter) model. Tangential patterns about the overdensities corresponding to clusters and groups of galaxies are apparent. A more complex network of patterns is also visible outside of these structures. The root-mean-square shear is approximately 2% in this map. (From Jain et al. 2000)

a standard Cold Dark Matter (SCDM) model is shown in Figure 3 for a $1 \times 1 \text{ deg}^2$ region. Jain, Seljak, & White (2000) derived this map from ray tracing through N-body simulations. Tangential patterns around the overdensities corresponding to clusters and groups of galaxies, along with a more complicated network of shear fluctuations, are apparent. By inverting the lensing equation (Equation 2), the shear map can be converted into a map of the projected mass κ and, therefore, of the dark matter distribution.

3 COSMIC-SHEAR STATISTICS AND COSMOLOGY

The statistical characteristics of the cosmic-shear field can be quantified using a variety of measures, which can then be used to constrain cosmological models. First, we consider the most basic two-point statistic of the shear field, namely the two-dimensional power spectrum (Jain & Seljak 1997, Kaiser 1998, Kamionkowski et al. 1997, Schneider et al. 1998a). The shear power spectrum C_1 is defined as a function of multipole moment l (or inverse angular scale) by $\sum_{i=1}^2 \langle \tilde{\gamma}_i(\mathbf{l}) \tilde{\gamma}_i(\mathbf{l}') \rangle = (2\pi)^2 \delta(\mathbf{l} - \mathbf{l}') C_1$, where tildes denote Fourier transforms (with the conventions of Bacon, Refregier, & Ellis 2000), δ is the two-dimensional Dirac-delta function, and

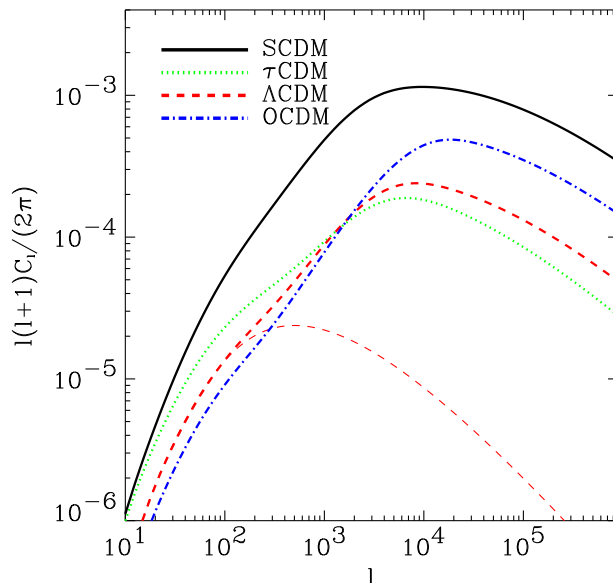


Figure 4: Shear power spectrum for different cosmological models and for source galaxies at $z_s = 1$. The SCDM model is COBE normalized and thus has a higher amplitude than the three cluster-normalized models Λ CDM, OCDM, and τ CDM. The thin dashed line shows the Λ CDM spectrum for linear evolution of structures. Notice that for $l > 1000$ (corresponding approximately to angular scales $\theta < 10'$) the lensing power spectrum is dominated by nonlinear structures.

the brackets denote an ensemble average. Applying Limber's equation in Fourier space (e.g., Kaiser 1998) to Equation 2 and using the Poisson equation, one can easily express the shear power spectrum C_l in terms of the three-dimensional power spectrum $P(k, \chi)$ of the mass fluctuations $\delta\rho/\rho$ and obtain

$$C_l = \frac{9}{16} \left(\frac{H_0}{c} \right)^4 \Omega_m^2 \int_0^{\chi_h} d\chi \left[\frac{g(\chi)}{ar(\chi)} \right]^2 P \left(\frac{l}{r}, \chi \right), \quad (4)$$

where a is the expansion parameter, and H_0 and Ω_m are the present value of the Hubble constant and matter density parameter, respectively. The lensing power spectra for four CDM models are shown in Figure 4 (see color insert) (see Bacon, Refregier & Ellis 2000 for the exact cosmological parameter values of each model). They were derived using the fitting formula for the nonlinear matter power spectrum $P(k, \chi)$ of Peacock & Dodds (1996). In Figure 4, the galaxies were assumed to lie on a sheet at a redshift $z_s = 1$. A more realistic redshift distribution $n(z)$ would require corrections of only approximately 10% on these power spectra, as long as the median redshift of the galaxies were kept at $z_s = 1$.

The three cluster-normalized models (Λ CDM, OCDM and τ CDM) yield power spectra of similar amplitudes but with different shapes. The COBE-normalized SCDM model has more power on a small scale and thus yields a larger normalization. For the Λ CDM model, the power spectrum corresponding to a linear evolution of structures is also shown in Figure 4 for comparison. For $l \gtrsim 1000$

(corresponding to angular scales smaller than approximately $10'$), nonlinear corrections dominate the power spectrum (Jain & Seljak 1997), making cosmic-shear sensitive to gravitational instability processes.

The measurement of the lensing power spectrum can thus be used to measure cosmological parameters, such as Ω_m , Ω_Λ , σ_8 , and Γ . (Bernardeau, van Waerbeke & Mellier 1997; Hu & Tegmark 1999; Jain & Seljak 1997; Kaiser 1998; van Waerbeke, Bernardeau & Mellier 1999). A full-sky cosmic-shear survey would yield a precision of these parameters comparable to that for future cosmic microwave background (CMB) missions. More realistically for the short term, a precision on the order of 10% can be achieved with surveys of approximately 10 square degrees. Such cosmic-shear surveys can also be combined with CMB anisotropy measurements to break degeneracies present when the CMB is considered alone (Hu & Tegmark 1999; Contaldi, Hoekstra & Lewis 2003). This would yield improvements in the precision of cosmological parameters by approximately one order of magnitude. In addition, the use of photometric redshifts can provide a tomographic measurement of matter fluctuations and improve the precision of cosmological parameters by up to an order of magnitude (Hu 1999, Hu & Keeton 2002, Taylor 2001).

In practice, it often is more convenient to measure other two-point statistics. In particular, the variance of the shear $\sigma_\gamma^2 \equiv \langle \bar{\gamma}^2 \rangle$ in randomly placed cells is widely used. It is related to the shear power spectrum by

$$\sigma_\gamma^2 = \frac{1}{2\pi} \int_0^\infty dl l C_l |\widetilde{W}_l|^2, \quad (5)$$

where \widetilde{W}_l is the Fourier transform of the cell aperture. The shear two-point correlation functions (eg. Kaiser 1998) are Fourier transforms of the power spectra and have also been measured by various groups (eg. Bacon et al. 2002; van Waerbeke et al. 2001a; Hoekstra et al. 2002a). The M_{ap} statistics (Schneider et al. 1998a) is another convenient statistic based on the average of the shear within a compensated filter. Its advantages are that its window function in l -space is narrow, that adjacent cells are effectively uncorrelated, and that it can be easily related to the statistics of the projected mass κ .

In analogy with electromagnetism, a tensor field like the shear field γ_i can be decomposed into an electric (E, or gradient) component and a magnetic (B, or curl) component (Crittenden et al. 2001b, Kaiser 1992, Kamionkowski et al. 1997, Stebbins 1996). Because the distortions it induces arise from a scalar field (the gravitational potential), weak lensing only produces E-type fluctuations. On the other hand, systematic effects and intrinsic galaxy alignments are likely to produce both E-type and B-type fluctuations (See Heavens 2001 for a review; also see Section 7.6). The presence of B-modes can thus be used as a measure of contaminants to the cosmic-shear signal. In practice, this decomposition can be performed using the M_{ap} statistic (Schneider et al. 1998a, van Waerbeke et al. 2001a) or the power spectrum (Hu & White 2000, Padmanabhan, Seljak & Pen 2002, Pen et al. 2001).

As is apparent in Figure 3, the shear field is not Gaussian but, instead, has apparent coherent structures. Bernardeau, van Waerbeke, & Mellier (1997) have shown that the skewness

$$S_3 = \frac{\langle \kappa^3 \rangle}{\langle \kappa^2 \rangle^2} \quad (6)$$

of the convergence field κ can be used to break the degeneracy between σ_8 and

Ω_m , which is present when the shear variance alone is considered. The measurement of higher-point statistics is thus of great cosmological interest, but their computation is made difficult by the fact that the angular scales accessible to observation ($\theta \lesssim 10'$) are in the nonlinear regime. Predictions for higher-point correlation functions have been calculated using perturbation theory, the hierarchical ansatz, (Bernardeau & Valageas 2000; Bernardeau, van Waerbeke & Mellier 1997; Hui 1999; Munshi & Coles 2000; Munshi & Jain 2001; van Waerbeke et al. 2001b) and halo models (Cooray & Hu 2001a; Cooray, Hu, & Miralda-Escudé 2000). These techniques have also been used to compute the full probability distribution function of the convergence field (Bernardeau & Valageas 2000, Munshi & Jain 2000, Valageas 2000) and the errors in two-point statistics (Cooray & Hu 2001b; Munshi & Coles 2002; Schneider et al. 2002).

Another possible way to compute the full nonlinear field is to use ray tracing through N-body simulations (Blandford et al. 1991; Hamana, Colombi & Mellier 2000; Jain, Seljak & White 2000; Premadi et al. 2001; Wambsganss, Cen, & Ostriker 1998; White & Hu 2000) to produce simulated shear maps such as those by Jain, Seljak & White (2000) (shown in Figure 3). These can be used to compute and study other proposed measures of non-Gaussianity such as peak statistics (Jain & van Waerbeke 2000), a generalized maximum likelihood (Taylor & Watts 2000), and cluster counts (Bartelmann, King & Schneider 2001). In practice, the complex geometry of surveys makes it difficult to infer a convergence κ map from the observed shear γ_i . For this reason, a number of researchers have recently proposed the use of high-order statistics of the shear field rather than the skewness S_3 of the convergence (Bernardeau, van Waerbeke, & Mellier 2003; Schneider & Lombardi 2002; Takada & Jain 2002; Zaldarriaga & Scoccimarro 2002).

4 SHEAR MEASUREMENT METHODS

Because the sought-after lensing signal is of only a few percent in amplitude, the data acquisition and analysis must be performed carefully, and systematic effects must be tightly controlled. All the current measurements of cosmic shear were derived from deep optical images taken with charged-coupled devices (CCD). It is advantageous for the exposures to be homogeneous in depth and for the ground to be subject to as small a seeing as possible. The fields are generally chosen to lie far away from each other to ensure that they are statistically independent and to minimize cosmic variance.

The first step in the data analysis is image processing. After flat fielding, the different exposures are co-added to produce the final reduced images. If necessary, any instrumental distortion induced by the telescope optics is corrected for at this stage. This can be done very accurately by measuring the astrometric offsets from several dithered exposures. For a detailed description of the different image-processing steps, see Kaiser et al. (1999). An example of a processed deep image from the cosmic-shear survey of Bacon, Refregier & Ellis (2000) is shown in Figure 5.

The next step consists of deriving an estimator for the shear from the shapes of the galaxies in the co-added images. The point-spread function (PSF), which smears the images of galaxies and is generally not circular, complicates this task. In general, the PSF varies spatially and in time, and it must be measured and

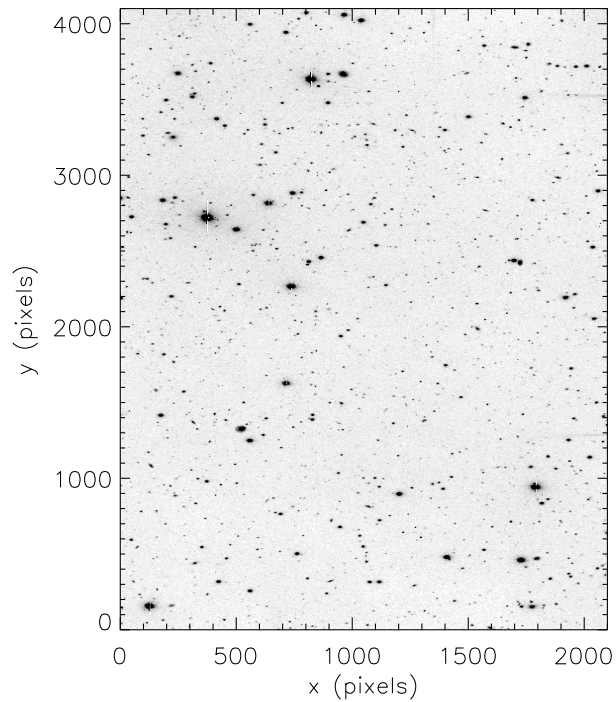


Figure 5: Example of an deep image in the cosmic-shear survey by Bacon, Refregier & Ellis (2000). This corresponds to a 1 h exposure with the EEV camera on the William Herschel Telescope (WHT). The field of view is $8' \times 16'$ and achieves a magnitude depth of $R \simeq 26$ (5σ detection). The bright objects are saturated stars. The faint objects comprise approximately 200 stars and approximately 2000 galaxies that are usable for the weak-lensing analysis. (From Bacon, Refregier & Ellis 2000)

modelled for each image individually. This can be done by measuring the shape of the stars in the field, whose number can be optimized by tuning the galactic latitudes of the observations. Figure 6 shows the ellipticity pattern of the PSF from one of the William Herschel telescope (WHT) fields of Bacon, Refregier & Ellis 2000.

Several methods have been developed to tackle this difficult and crucial task. The more rigorous method of Kaiser, Squires & Broadhurst (KSB; 1995), further developed by Luppino & Kaiser (1997) and Hoekstra et al. (1998), replaced the earlier method by Bonnet & Mellier (1995). The KSB method is now widely used for cluster studies, and it has been used by the majority of the groups involved in measuring cosmic shear (see Bartelmann & Schneider 1999 for a detailed review of the KSB method). It is based on the measurement of the quadrupole moment of the galaxy surface brightness $I(\mathbf{x})$,

$$Q_{ij} \equiv \int d^2x x_i x_j w(x) I(\mathbf{x}), \quad (7)$$

where $w(x)$ is a weight function conveniently taken to be Gaussian. These moments capture the lowest-order shape information of the galaxy and can be combined to form the ellipticity of the galaxy

$$\epsilon_1 = \frac{Q_{11} - Q_{22}}{Q_{11} + Q_{22}}, \quad \epsilon_2 = \frac{2Q_{12}}{Q_{11} + Q_{22}}. \quad (8)$$

The first (second) component of the ellipticity describes compressions and elongations along (at 45° from) the x and y axes (see Figure 2 for an illustration). The ellipticity vanishes for circular galaxies.

The first step in the KSB method is to correct the observed galaxy ellipticity $\epsilon_i^{g'}$ for the anisotropy of the PSF. The corrected galaxy ellipticity ϵ^g is given by

$$\epsilon^g = \epsilon^{g'} - P_{\text{sm}}^g (P_{\text{sm}}^*)^{-1} \epsilon^*, \quad (9)$$

where ϵ^* is the PSF ellipticity derived from the stars, and P_{sm}^g and P_{sm}^* are the smear susceptibility tensors for the galaxy and star, respectively, and can be derived from higher moments of the images. The shear in a patch of the sky can then be measured by averaging over the (corrected) ellipticities in the patch of the sky using

$$\gamma = (P_\gamma)^{-1} \langle \epsilon^g \rangle, \quad (10)$$

where the tensor P_γ quantifies the susceptibility to shear acting before isotropic PSF smearing and is given by

$$P_\gamma = P_{\text{sh}}^g - P_{\text{sh}}^* (P_{\text{sm}}^*)^{-1} P_{\text{sm}}^g, \quad (11)$$

where the shear susceptibility tensors P_{sh}^g and P_{sh}^* for the galaxies and the stars can also be measured from higher moments of their respective light distribution.

The KSB method was thoroughly tested using realistic simulated images by Erben et al. (2001) and Bacon et al. (2001a). These studies showed that it is accurate to within a few tenths of percent in reconstructing an input shear and is thus sufficient for the current cosmic-shear surveys (see Section 5). However, this accuracy is insufficient for future, more sensitive surveys (see Section 6). Moreover, Kuijken (1999) and Kaiser (2000) have shown that the KSB method is ill-defined mathematically and unstable for PSF's found in practice.

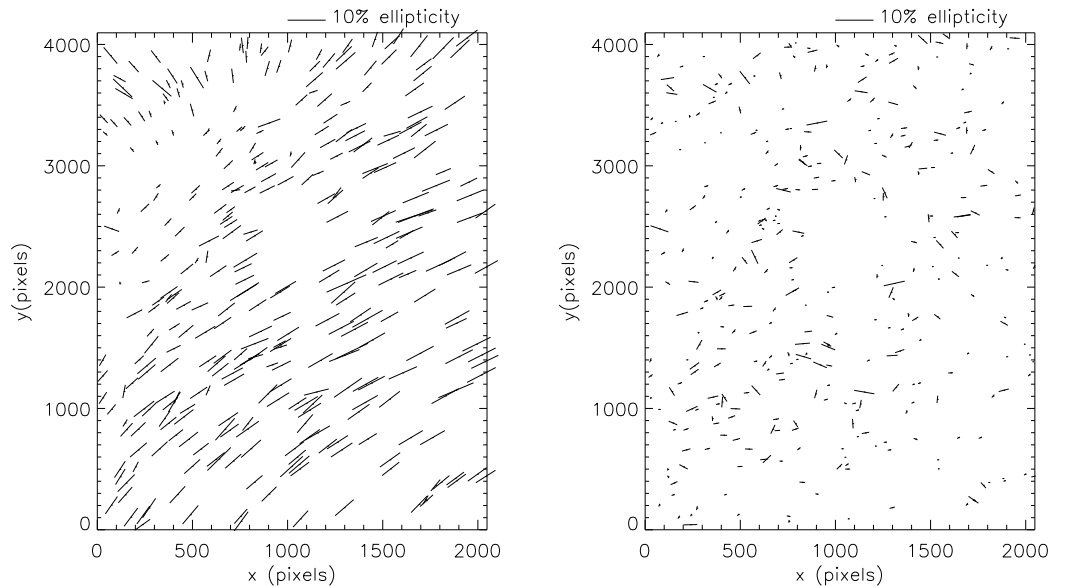


Figure 6: PSF ellipticity pattern measured in WHT field shown in the Figure 5: (a) PSF ellipticities measured from the stars in Figure 5. (b) Ellipticity residuals for those stars after the KSB corrections. In this survey, the root-mean-square stellar ellipticity is found to be approximately 7% before the corrections and negligible after the correction. (From Bacon, Refregier & Ellis 2000)

This inadequacy has led a number of researchers to develop alternative methods. Rhodes, Refregier & Groth (2000) have modified the KSB method to be better suited for HST images. Kuijken (1999) considered a different approach that consisted of fitting the observed galaxy shape with a smeared and sheared circular model. Kaiser (2000) introduced a new method based on a finite resolution shear operator. Refregier & Bacon (2003) and, independently, Bernstein & Jarvis (2001) developed a new method based on the decomposition of the galaxies into shape components or “shapelets”. The gauss-hermite orthogonal basis functions used in this approach allow shears and PSF convolutions to be described as simple matrix operations, using the formalism developed for the quantum harmonic oscillator (Refrégier 2003). These new methods are promising but require extensive testing to establish whether they will achieve the required precision.

5 OBSERVATIONS

Because the expected distortions are only of a few percent, the measurement of cosmic shear requires large survey areas and excellent image quality. Early searches for cosmic shear signals with photographic plates were unsuccessful (Kristian 1967; Valdes, Jarvis & Tyson 1983). Mould et al. (1994), performed the first attempt to detect a cosmic-shear signal with CCDs, but only derived an upper limit. Using the same data, Villumsen (1995) reported a 4.5σ detection. Schneider et al. (1998b) then reported a detection of cosmic shear in one of three QSO fields, an area too small to draw any constraints on cosmology.

Within a few weeks, four independent groups (Bacon, Refregier & Ellis 2000;

Kaiser, Wilson & Luppino 2000; van Waerbeke et al. 2000; Wittman et al. 2000) reported the first firm statistical detections of cosmic shear using three different 4-m-class telescopes: the Cerro Tololo Inter-American Observatory (CTIO), the Canada-France-Hawaii Telescope (CFHT), and the William Herschel Telescope (WHT). These were later confirmed by more precise measurements of the cosmic-shear amplitude from the ground (Bacon et al. 2002; Brown et al. 2003; Maoli et al. 2001; Hamana et al. 2003; Hoekstra et al. 2002a; Hoekstra, Yee & Gladders 2002a; Jarvis et al. 2002; van Waerbeke et al. 2001; van Waerbeke et al. 2002a) using 2-m – (MPG/ESO), 4-m– (WHT, CFHT, CTIO) and 8-m– (Very Large Telescope, Keck, Subaru) class ground-based telescopes. Meanwhile, cosmic shear was also detected (Hämmerle et al. 2002; Rhodes, Refregier & Groth 2001) and measured (Refregier, Rhodes & Groth 2002) from space using HST. Space-based surveys are currently limited by the small field of view of HST, but they are deeper and less prone to systematics thanks to the absence of atmospheric seeing.

Table 1 summarizes the existing cosmic-shear surveys and highlights the wide range of telescopes, survey areas, and depths. The shear variance σ_γ^2 (Equation 5) measured recently by several groups is shown in Figure 7 (see color insert) as a function of the radius a circular cell. The results by Hämmerle et al. (2002) and Hamana et al. (2002a) are not displayed. Note that, for the shear variance, the data points at different angular scales are not independent. For comparison, the shear variance predicted for a Λ CDM model with $\sigma_8 = 1$ is also shown in Figure 7. The model is displayed for median galaxy redshifts of z_m from 0.8 to 1.0, corresponding approximately to the range of depths of the top five surveys displayed (van Waerbeke et al. 2002a; Brown et al. 2003; Bacon et al. 2002, WHT and Keck; Refregier et al. 2002). These observations are approximately consistent with each other and with the Λ CDM model on angular scales from 0.7 to 20 arcmins. This is compelling given that these were performed with different telescopes (and therefore different instrumental systematics) and independent data-analysis pipelines.

The bottom two surveys (Hoekstra et al. 2002b; Jarvis et al. 2002) have a median redshift in the range $z_m \simeq 0.6$ – 0.7 and yield lower shear variances. As indicated by the theoretical curves in figure 7, this redshift dependence is expected in CDM models and thus confirms the detection of a cosmic shear signal.

Although the shear variance was displayed for the purpose of Figure 7, some of the groups have used instead the shear correlation function or M_{ap} statistic to quantify their lensing signal. Recently, several groups used the latter statistic to separate their signal into E and B components (see Section 3) and thus to estimate and subtract systematic effects (Jarvis et al. 2002; Hamana et al. 2003; Hoekstra, Yee & Gladders 2002; van Waerbeke et al. 2001, 2002a). Pen, van Waerbeke & Mellier (2001) and Brown et al. (2003) chose instead to measure directly the shear power spectrum for each E and B mode. Figure 8a shows the measurement of the E and B signals using the M_{ap} statistic by Hoekstra, Yee & Gladders (2002a), for several R_c -magnitude ranges in the Red-Sequence Cluster (RCS) survey. They measure a clear lensing signal apparent as E modes. However, the significant B modes reveals the presence of residual systematics on small scales ($\theta \lesssim 10'$), especially for bright galaxies. In their analysis, these authors use the amplitude of the B modes as a measure systematic uncertainties.

Existing cosmic-shear measurements already yield interesting constraints on the amplitude of the matter power spectrum σ_8 on which the lensing signal strongly depends. For instance, Figure 8b shows cosmological constraints for

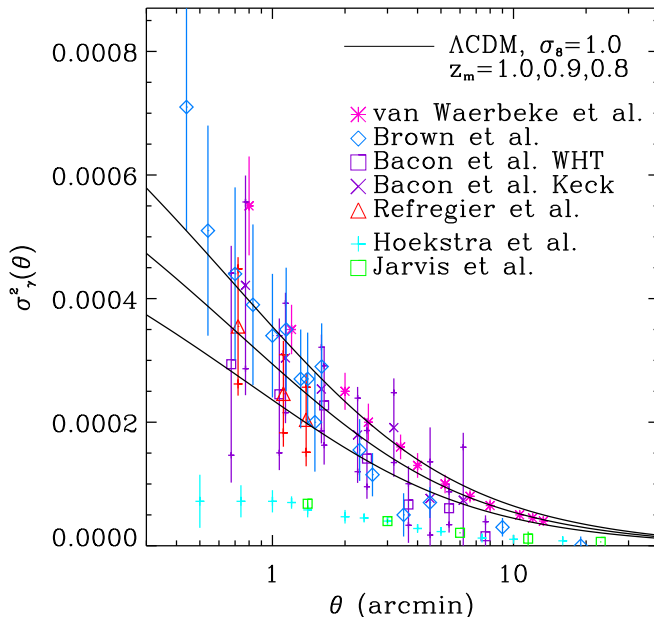


Figure 7: Shear variance σ_γ^2 as a function of the radius θ of a circular cell. The data points correspond to recent results from different groups: van Waerbeke et al. (2002a), Brown et al. (2003), Bacon et al. (2002, WHT and Keck), Refregier et al. (2002), Hoekstra et al. (2002b), Jarvis et al. (2002). When relevant, the inner error bars correspond to noise only, whereas the outer error bars correspond to the total error (noise + cosmic variance). The measurements by Hämmerle et al. (2002) and Hamana et al. (2003) are not displayed. The solid curves show the predictions for a Λ CDM model with $\Omega_m = 0.3$, $\sigma_8 = 1$, and $\Gamma = 0.21$. The galaxy median redshift was taken to be $z_m = 1.0, 0.9$, and 0.8 , from top to bottom, respectively, corresponding approximately to the range of depth of the top five surveys. The bottom two surveys (Hoekstra et al. 2002b; Jarvis et al. 2002) have a median redshift in the range $z_m \simeq 0.6-0.7$ and, as expected, yield lower shear variances.

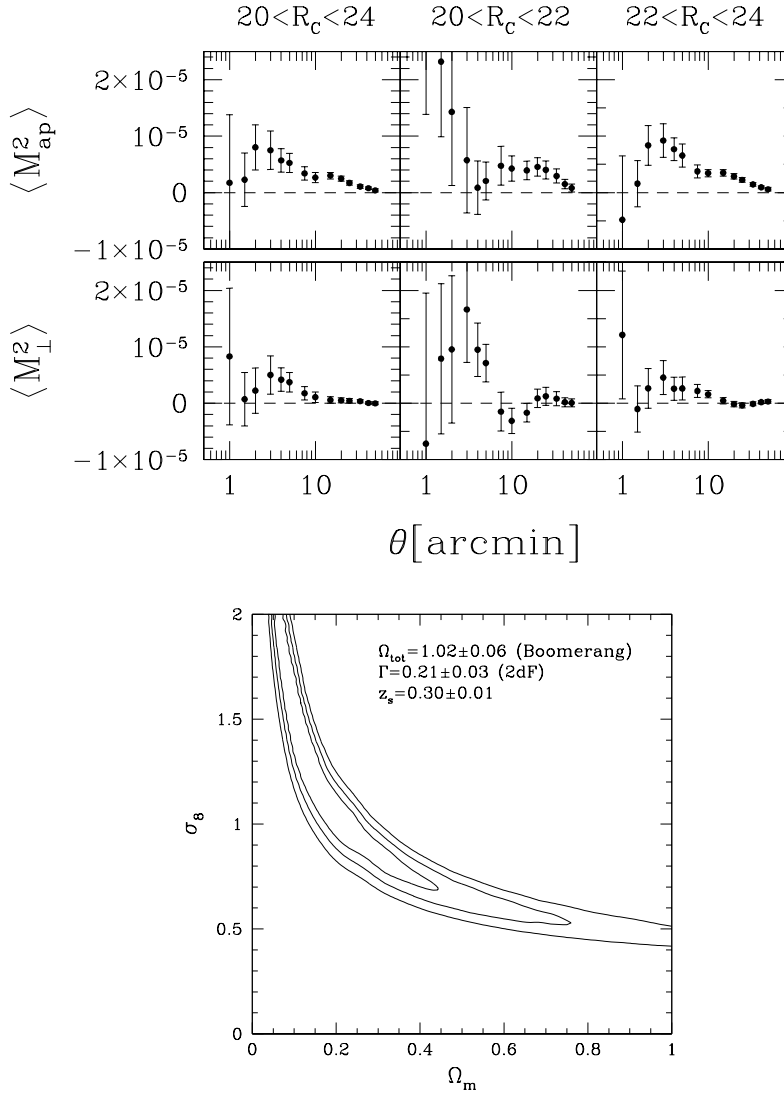


Figure 8: Cosmic shear measurement by Hoekstra, Yee & Gladders (2002a) from the RCS survey. (a): measurement of the E (top panels) and B (bottom panels) modes of the M_{ap} statistics variance as a function of aperture scale θ . Several ranges of the R_c -magnitude are considered. The errors correspond to 1σ statistical uncertainties. The presence of significant B Modes reveal the presence of residual systematics on small scales ($\theta \leq 10'$). (b): Cosmological constraints derived from their measurement of the E -mode M_{ap} statistics for $22 < R_c < 24$ after accounting for the residual B -modes. The joint constraints are shown for Ω_m and σ_8 in the Λ CDM model. Priors from CMB and galaxy surveys were used to marginalize over Ω_{tot} , Γ , and the source redshift z_s . The contours indicate 68.3%, 95.4%, and 99.9% confidence levels. (From Hoekstra, Yee & Gladders 2002a)

Table 1: current cosmic-shear surveys

Reference	Telescope	Area (deg ²)	Mag. limit	σ_8^a
Wittman et al. 2000	CTIO	1.0	$R \lesssim 26$	
van Waerbeke et al. 2000	CFHT	1.7		
Kaiser et al. 2000	CFHT	0.96	$I \lesssim 24, V \lesssim 25$	
Bacon et al. 2000	WHT	0.5	$R \lesssim 26$	$1.50^{+0.50}_{-0.50}$
Maoli et al. 2001	VLT	0.65	$I \lesssim 24.5$	$1.03^{+0.03b}_{-0.03}$
Rhodes et al. 2001	HST/WFPC2	0.05	$I \lesssim 26$	$0.91^{+0.25}_{-0.30}$
van Waerbeke et al. 2001a	CFHT	6.5	$I \lesssim 24.5$	$0.88^{+0.02c}_{-0.02}$
Hämmerle et al. 2002	HST/STIS	0.02		
Hoekstra et al. 2002a	CFHT, CTIO	24	$R \lesssim 24$	$0.81^{+0.07}_{-0.09}$
van Waerbeke et al. 2002a	CFHT	8.5	$I \lesssim 24.5$	$0.98^{+0.06}_{-0.06}$
Refregier et al. 2002	HST/WFPC2	0.36	$\langle I \rangle \simeq 23.5$	$0.94^{+0.14}_{-0.14}$
Bacon et al. 2002	WHT, Keck	1.6	$R \lesssim 26$	$0.97^{+0.13}_{-0.13}$
Hoekstra et al. 2002b	CFHT, CTIO	53	$R \lesssim 24$	$0.86^{+0.04}_{-0.05}$
Brown et al. 2003	MPG/ESO	1.25	$R \lesssim 25$	$0.72^{+0.09}_{-0.09}$
Hamana et al. 2003	Subaru	2.1	$R \lesssim 26$	$0.69^{+0.18}_{-0.13}$
Jarvis et al. 2002	CTIO	75	$R \lesssim 23$	$0.71^{+0.06}_{-0.08}$

^afor Λ CDM model with $\Omega_m = 0.3$, $\Omega_\Lambda = 0.7$; Γ is marginalised over or set to 0.21 when possible; errors correspond to 68%CL

^bfor combination of Maoli et al. (2001), van Waerbeke et al. (2000), Bacon et al. (2000), and Wittman et al. (2000); cosmic variance not included.

^ccosmic variance not included.

a Λ CDM model derived by Hoekstra, Yee & Gladders (2002a) from the measurement of the M_{ap} statistic for their $22 < R_c < 24$ galaxy sample. The degeneracy between σ_8 and Ω_m apparent in the figure is typical of cosmic-shear measurements involving only two-point statistics. Hoekstra, Yee & Gladders (2002a) found that the constraints are well described by $\sigma_8 \Omega_m^{0.52} = 0.46^{+0.05}_{-0.07}$ (95% CL), where priors from CMB and galaxy survey data have been used to marginalize over Γ and Ω_Λ . Other surveys find constraints of the same form with similar exponents for Ω_m .

Table 1 lists the values of σ_8 found by the different groups. The errors have been converted to 68% confidence level (CL) when necessary, and values of $\Omega_m = 0.3$, $\Omega_\Lambda = 0.7$, and $\Gamma = 0.21$ have been assumed, when possible. The most recent values are displayed in Figure 9 (see color insert), along with their average $\sigma_8 \simeq 0.83 \pm 0.04$ (1σ). The values derived by the different cosmic shear groups are in the range $\sigma_8 \simeq 0.7$ – 1.0 , with the most recent measurements (Brown et al. 2003; Hamana et al. 2003; Jarvis et al. 2002) yielding lower values. The 2– 3σ mutual inconsistencies between some of the measurements may be symptomatic of a small level of residual systematics. In particular, calibration errors in the shear measurement method would not be detected via the E - B decomposition and are a likely explanation (see Hirata & Seljak 2003). Another source of discrepancy arises from the different fitting functions for the non-linear evolution of the power spectrum (see section 2). Apart from Brown et al. (2003; see also Contaldi et al. 2003) who used the more accurate results of Smith et al. (2003), the other groups used the Peacock & Dodds (1997) fitting function which yields an underprediction of σ_8 by roughly 5–10%. The impact of these systematics will be discussed further in section 7.

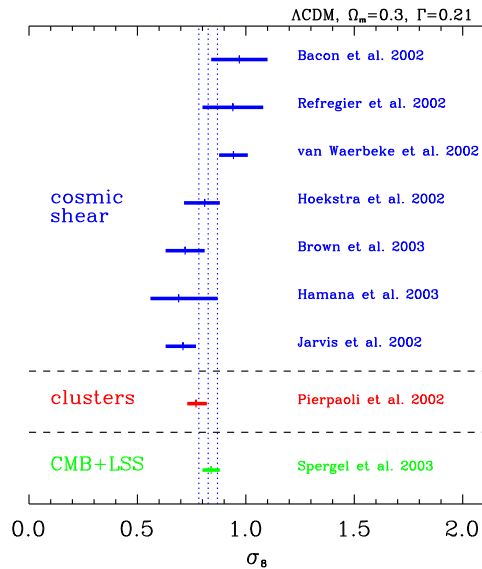


Figure 9: Comparison of the determination of σ_8 by different groups and methods. The errors have all been converted to 1σ , and a Λ CDM model with $\Omega_m = 0.3$ and $\Gamma = 0.21$ was assumed when possible. The vertical dotted lines show the average $\sigma_8 \simeq 0.83 \pm 0.04$ of the seven cosmic-shear measurements and associated 1σ error. The normalization from cluster abundance (e.g., Pierpaoli et al. 2002) as well as that derived from CMB anisotropies and local large-scale structure (galaxy and Lyman α surveys; Spergel et al. 2003) are also shown.

Interestingly, an independent measurement of σ_8 is provided by the abundance of X-ray clusters and can be directly compared to this value. Initially, this method yielded normalisations of $\sigma_8 \sim 0.9$ (Eke et al. 1998; Pierpaoli, Scott & White 2001; Viana & Liddle 1999), in agreement with the early cosmic shear results (see table 1 and figure 9). This value was subsequently revised downward to $\sigma_8 \sim 0.7\text{--}0.8$ by the use of the observed, rather than simulated, mass-temperature relation in clusters (Borgani et al. 2001; Reiprich & Böhringer 2001; Seljak 2001; Viana, Nichol & Liddle 2001; Pierpaoli, Scott & White 2002). Recently, Spergel et al. (2003) derived a value of $\sigma_8 = 0.84 \pm 0.04$ (68%CL) from a joint analysis of CMB anisotropy measurements from the Wilkinson Microwave Anisotropy Probe (WMAP) and other experiments, galaxy clustering and the Lyman α forest. For comparison, these results along with a representative value of the revised cluster-abundance normalization (Pierpaoli, Scott & White 2002) are also shown in figure 9. The average of the cosmic shear results is formally in good agreement with the determination of σ_8 using the other techniques. Future surveys are however needed to confirm this, by resolving the discrepancies between the current cosmic shear measurements. Also, a full likelihood analysis would be required to establish the significance of the agreement between the different techniques (see Contaldi et al. 2003). This comparison is important as it provides a strong test of the Λ CDM model, the gravitational instability paradigm, the physics of clusters, and of the biased formation of galaxies.

As discussed in Section 3, the degeneracy between σ_8 and Ω_m can be broken by measuring higher-order correlation functions of the lensing field. Bernardeau,

Mellier, & van Waerbeke (2002) recently reported the first detection of a non-Gaussian shear signal using the 3-point shear correlation function formalism of Bernardeau, van Waerbeke & Mellier (2003). Another measure of non-gaussianity was recently performed by Miyazaki et al. (2002) using peak statistics in their Subaru survey. Although these results are consistent with that expected from structure formation models, larger survey areas are needed to infer cosmological constraints.

Another approach to probe the dark matter is to measure the bias between the mass and galaxies by cross-correlating the shear map with that of the light from foreground galaxies in the same region of the sky (Cooray 2002, Schneider 1998, van Waerbeke 1998). Hoekstra, Yee & Gladders (2001a), Hoekstra et al. (2002b), and Wilson, Kaiser & Luppino (2001) have recently measured this cross-correlation on large scales.

6 FUTURE SURVEYS AND PROSPECTS

The existing measurements described above are primarily limited by statistics. They will therefore be improved upon by ongoing surveys on existing telescopes, such as the Legacy Survey on CFHT (CFHTLS; Mellier et al. 2000), the Deep Lens Survey (Wittman et al. 2002), surveys with the Subaru telescope (Hiroyasu et al. 2001) and the Sloan Digital Sky Survey (Stebbins, McKay & Frieman 1995). Future instruments dedicated to surveys and for which cosmic shear is a primary science driver are being planned, such as Megacam on CFHT (Boulade et al. 2000), the Visible and Infrared Survey Telescope for Astronomy (VISTA; Taylor et al. 2003), the Large aperture Synoptic Survey Telescope (LSST; Tyson et al. 2002a,b), or the novel Panoramic Survey Telescope and Rapid Response System (Pan-STARRS; Kaiser, Tonry & Luppino 2000). From space, the new Advanced Camera for Surveys (ACS) on HST and, much more ambitiously, the future Supernova Acceleration Probe satellite (SNAP; Perlmutter et al. 2003; Rhodes et al. 2003; Massey et al. 2003; Refregier et al. 2003) also offer exciting prospects. Table 2 lists the characteristics of some of these future surveys. Broadly speaking, ground-based measurements will cover large areas, whereas space-based surveys will yield higher-resolution maps and reduced systematics thanks to the absence of atmospheric seeing.

Radio surveys offer another interesting prospect. Ongoing efforts are aimed at detecting cosmic shear with the FIRST radio survey (Chang & Refregier 2002, Kamionkowski et al. 1997, Refregier et al. 1998). The future radio telescopes LOFAR (Low Frequency Array) and SKA (Square Kilometer Array) will yield cosmic-shear measurements of comparable sensitivity to the most ambitious optical surveys (Schneider 1999). The advantages of radio surveys are that they cover large solid angles, that the bright radio sources are at a higher redshift, and that the PSF is fully predictable and reproducible.

These future surveys will provide very accurate measurements of cosmological parameters through the measurement of the lensing power spectrum and higher-order statistics. Figure 10 (see color insert) shows, for instance, the excellent accuracy with which the lensing power spectrum will be measured with the SNAP wide survey. They will also allow us to test some of the foundations of the standard cosmological model. For example, the measurement of the power spectrum on nonlinear scales at different redshift slices, and of the hierarchy of

Table 2: Future cosmic-shear surveys

Telescope/Survey	Ground/Space	Diameter (m)	FOV (deg ²)	Area (deg ²)	Start ^a	Ref. ^b
DLS	ground	2×4	2×0.3	28	1999 ^c	1
CFHTLS	ground	3.6	1	172	2003	2
VST	ground	2.6	1	$x100^d$	2004	3
VISTA ^e	ground	4	2	10000	2007	4
Pan-STARRS	ground	4×1.8	4×4	31000	2008	5
LSST	ground	8.4	7	30000	2012	6
SNAP	space	2	0.7	300	2011	7

^a planned start date of the cosmic shear surveys

^b references: 1: Wittman et al. 2002; 2: Mellier et al. 2000; 3: Kuijken et al. 2002; 4: Taylor et al. 2003; 5: Kaiser et al. 2000; 6: Tyson et al. 2002a,b; 7: Perlmutter et al. 2003, Rhodes et al. 2003, Massey et al. 2003, Refregier et al. 2003

^c the survey will be complete in 2003

^d a survey of several 100 deg² is planned

^e assuming the availability of the optical camera

high-order correlation functions, will yield a direct test of the gravitational instability paradigm. The lensing power spectrum can also be used to measure the equation of the state of the dark energy w and thus complement supernovae measurements in the constraining of quintessence models (Benabed & Bernardeau 2001; Hui 1999; Huterer 2001; Hu 2001, 2002; Munshi & Wang 2002; Weinberg & Kamionkowski 2002). Figure 10 shows, for instance, that a change of 40% in w can easily be measured by SNAP (see Refregier et al. 2003). Cosmic-shear measurements can also be used to test general relativity (Uzan & Bernardeau 2001).

Another promising approach to measure weak lensing is to use the fluctuations of the CMB temperature as the background sources (Bernardeau 1997, 1998; Cooray & Kesden 2002; Hirata & Seljak 2002; Hu 2000; Seljak 1996; Seljak & Zaldarriaga 1999; Zaldarriaga & Seljak 1998). Because these fluctuations are produced at a redshift of approximately 1100, CMB lensing provides a probe of the evolution of mass fluctuations at redshifts larger than those probed by optical galaxies. Lensing indeed produces distinct non-Gaussian signatures that can be used to reconstruct the foreground mass distribution and probe the growth of structures. This approach will become feasible with the advent of future CMB missions such as Planck Surveyor or ground-based instruments with high angular resolutions.

7 CHALLENGE: SYSTEMATIC EFFECTS

For the future surveys described above to yield their full potential, a number of challenges must be met. Indeed, these surveys require the measurement of shears on the order of 1% with an accuracy better than 0.1%; thus, they require a very tight control of systematic effects. In the following, we review the main sources of systematics.

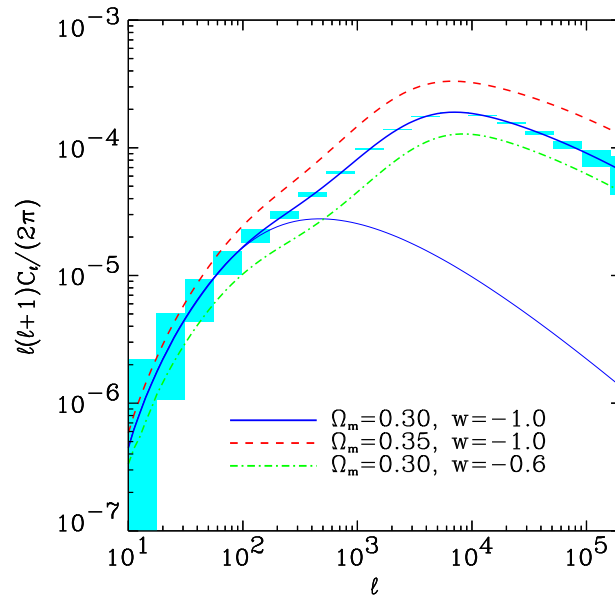


Figure 10: Prospects for the measurement of the weak-lensing power spectrum with future weak-lensing surveys. The solid line represents the lensing power spectrum of a Λ CDM model with $\Omega_m = 0.3$ (and an equation of state $w = -1$). The boxes correspond to the band-averaged 1σ errors for the SNAP wide survey (300 deg^2 , 100 galaxies per arcmin^2 with a root-mean-square intrinsic ellipticity dispersion of $\sigma_\epsilon = 0.31$). The precision is highest in the nonlinear region [see the linear Λ CDM power spectrum (*dotted line*)] and will thus provide a test of the gravitational instability paradigm. This model can easily be distinguished from models that differ from it by a 17% change in Ω_m (*dashed line*) or by a 40% change in the dark-energy equation of state w (*dot-dashed line*).

7.1 *PSF Anisotropy*

The most serious systematic for ground-based surveys is that produced by the rather large PSF ellipticities ($\sim 10\%$) observed by the different groups. The KSB method (see Section 4) provides a correction of the PSF anisotropy by, at most, a factor of approximately 10, which is insufficient for a precision of 0.1% in shear. Although new shear measurement methods may improve upon this (see Section 4 and below), the correction is fundamentally limited by the finite surface density and signal-to-noise ratio of the stars used to measure the PSF shape. It is, therefore, necessary for the PSF ellipticity to be reduced in hardware as well as in software. This can be done by using tighter constraints in the tracking and optical systems of the new telescopes and instruments as well as with interactions between telescope designers, engineers, and scientists.

7.2 *Shear Measurement Method*

Even if the PSF ellipticity were guaranteed to be isotropic, future measurements will be limited by the precision of the shear measurement methods. The KSB method is accurate to measure shears of approximately 1% with only a 10% accuracy (Bacon et al. 2001, Erben et al. 2001). This will soon become an important limiting factor (see Hirata & Seljak 2003). Although new methods (see Section 4) promise to improve upon this, more extensive simulations are required to establish that the same accuracy can be reached for shears of 0.1%.

7.3 *Redshift Distribution*

To convert cosmic-shear measurements into constraints on cosmological parameters, the redshift distribution of the background galaxies must be known (see Section 4). The uncertainty in the median galaxy redshift is already one of the dominant contributions to the uncertainty in the amplitude of the matter power spectrum from cosmic shear. The determination of the galaxy redshift distribution is made difficult by the depth of the cosmic-shear surveys. In addition, the sample of galaxies is not simply magnitude limited, but it is subject to complex selection cuts throughout the shear measurement pipeline. Dedicated spectroscopic surveys and photometric redshift studies (such as that by Brown et al. 2003) are thus required to overcome this limitation.

7.4 *CCD Nonlinearities*

All the shear measurement methods rely on the assumption that the instrumental response is linear. It is therefore important to test whether CCD cameras do not have subtle pixel-to-pixel nonlinearities that would induce biases in the shear measurements. The mean shear offset and the shear gradient across the chip found by van Waerbeke et al. (2001) could be due to this effect.

7.5 *Overlapping Isophotes*

Two neighboring galaxies in an image yield "peanut-shaped" isophotal contours and thus appear to have aligned ellipticities. This overlapping-ellipticities effect may produce a spurious ellipticity correlation signal on small scales. van Waerbeke et al. (2000) suggested that this effect may explain the excess shear signal,

which they measured on small scale and which disappeared when close pairs were discarded. Evidence for this effect was also found in the image simulation by Bacon et al. (2001). More extensive and detailed simulations would need to be performed to ascertain and calibrate this effect.

7.6 *Intrinsic Correlations*

The measurement of the lensing shear relies on the assumptions that, in the absence of lensing, the ellipticities of the galaxies are uncorrelated. However, an intrinsic correlation of galaxy shapes could exist owing to the coupling of the galaxy angular momentum or shape to the tidal field or to galaxy interactions (see Heavens 2001 for a review). Theoretical estimation of the size of this effect has been performed using numerical simulations (Croft & Metzler 2000; Heavens, Refregier & Heymans 2000; Jing 2002) and analytical methods (Catalan, Kamionkowski & Blandford 2001; Crittenden et al. 2001a,b; Lee & Pen 2001; Mackey, White & Kamionkowski 2001). Measurements of intrinsic correlations have also been performed (Brown et al. 2000; Pen, Lee & Seljak 2000). Although considerable uncertainty remains regarding the amplitude of this effect, a consensus is arising that intrinsic correlations are likely to be small for the deep current surveys with $z_m \sim 1$, but may be dominant for shallower surveys with $z_m \lesssim 0.2$ (see however the conflicting results of Jing 2002). Although lensing distortions are coherent over a large redshift range, intrinsic alignments are only significant for small physical separations. Photometric redshifts can thus be used to separate and reduce intrinsic correlations from cosmic-shear signals (Heymans & Heavens 2002; King & Schneider 2002a,b). Another approach is to search for the B -type correlation signal produced by intrinsic correlations (Crittenden et al. 2001b).

7.7 *Theoretical Uncertainties*

Most of the signal in cosmic-shear surveys arises from small scales ($\theta \lesssim 10'$) and thus from nonlinear structures (Jain & Seljak 1997). The existing prescriptions for computing the nonlinear corrections (Peacock & Dodds 1997; Ma 1998) to the matter power spectrum are only accurate to approximately 10% and disagree at that level with one another (see discussion in Huterer 2001). This theoretical uncertainty will soon become one of the dominating errors in the determination of cosmological parameters from cosmic-shear surveys (see discussion in van Waerbeke et al. 2002). New prescriptions based on more recent N-body simulations such as those by Smith et al. (2003) will help improve the accuracy of the predictions. The problem of the prediction of higher-order statistics is even more difficult, but it is not as pressing given the large uncertainties in the measurements within current surveys (see Bernardeau, Mellier, van Waerbeke 2002). The inclusion of second-order terms in the weak-lensing approximation will eventually also be required (Cooray 2002, Cooray & Hu 2002).

These systematic effects must be controlled to match the statistical accuracy of future surveys. Along with the studies suggested above, further measurements with different colors and comparison of various surveys in overlapping regions would help to control systematics and to test data analysis pipelines. On the theoretical side, larger simulations coupled with advanced analytical techniques will be required.

8 CONCLUSIONS

Cosmic shear has emerged as a powerful method to measure the large-scale structure in the universe. It can be thought of as the measurement of background fluctuations in the space-time metric. Although other methods rely on assumptions relating the distribution of light to that of the mass, weak lensing is based on “clean” physics and can be directly compared to theory. The past three years have yielded impressive observational progress, as the first statistical detections and measurements of cosmic shear have been achieved. In analogy with the CMB, cosmic shear has moved from the COBE era to that of the first generation of anisotropy experiments. However, the measurement of cosmic shear differs from that of CMB anisotropies in several respects. First, the fluctuations are on the order of 10^{-2} as opposed to 10^{-5} , making them easier to measure while retaining the validity of linear calculations. Second, the cosmic-shear field is non-Gaussian and therefore contains more information than that quantified by the power spectrum.

Existing cosmic-shear measurements have started to yield significant constraints on cosmological parameters. The measurement of the amplitude of the matter power spectrum $\sigma_8\Omega_m^{0.5}$ from cosmic shear should soon replace that derived from the local abundance of clusters. This latter technique is indeed limited by the finite number of bright clusters and by systematic uncertainties in the physics of clusters. With better statistics, the angular and redshift dependence of the shear signal as well as with higher-order moments of the convergence field will break the degeneracy between σ_8 and Ω_m and yield constraints on further parameters such as Ω_Λ and Γ .

The current measurements of cosmic shear are now primarily limited by statistics. They will therefore be improved upon by a number of upcoming and future instruments such as Megacam, VST, VISTA, LSST, and Pan-STARRS from the ground, and HST/ACS and SNAP in space. For several of these instruments, a weak-lensing survey has been listed as one of the primary science drivers. These surveys will potentially yield measurements of cosmological parameters that are comparable in precision and complementary to those derived from the CMB. They will also be able to address more far-reaching questions in cosmology by measuring parameters beyond the standard model. For instance, they can be used to provide a test of the gravitational instability paradigm, a measure of the equation of state of the dark energy, and a test of general relativity.

For these instruments to yield the full promise of cosmic shear, a number of challenges have to be met. First, observationally, systematic effects, such as the PSF anisotropy and CCD nonlinearities, must be controlled and corrected for. From the theoretical point of view, calculations of the nonlinear power spectrum, of high-order statistics, and of the associated errors must be improved to meet the precision of future measurements. The observational and theoretical efforts required to overcome these difficulties are worthwhile given the remarkable promise that cosmic shear offers to cosmology.

ACKNOWLEDGMENTS The author thanks his collaborators David Bacon, Richard Massey, Tzu-Ching Chang, Jason Rhodes, and Richard Ellis for numerous fruitful discussions. The author thanks Bhuvnesh Jain, David Bacon, and Henk Hoekstra for their permission to reproduce their figure. He also thanks Tony Tyson, Hervé Aussel and Andy Taylor for precisions regarding the parameters of future cosmic shear surveys. He is also grateful to Richard Ellis, Henk Hoekstra, Gary Bern-

stein, Yannick Mellier, Richard Massey, and Ivan Valtchanov for useful comments on the manuscript.

The Annual Review of Astronomy and Astrophysics is online at
<http://astro.annualreviews.org>

Literature Cited

- Babul, A Lee MH. 1991. *MNRAS* 250:407
 Bartelmann M, King LJ, Schneider P. 2001. *Astron. Astrophys.* 378:361
 Bartelmann M, Schneider P. 1999. astro-ph/9912508
 Bacon DJ, Refregier A, Clowe D, Ellis R. 2001. *MNRAS* 325:1065
 Bacon DJ, Refregier A, Ellis R. 2000. *MNRAS* 318:625
 Bacon DJ, Massey R, Refregier A, Ellis R. 2002. astro-ph/0203134
 Benabed K, Bernardeau F. 2001. *Phys. Rev. D* 64:083501
 Bennet DP, Rhie SH. 2000. *GEST Home Page*.
<http://bustard.phys.nd.edu/GEST>. astro-ph/0011466
 Bernardeau F. 1997. *Astron. Astrophys.* 324:15
 Bernardeau F. 1998. *Astron. Astrophys.* 338:767
 Bernardeau F. 1999. Theoretical and Observational Cosmology. *Proc. Cargese Summer Sch., Cargese, France*, ed. M Lachieze-Rey. astro-ph/9901117
 Bernardeau F, Mellier Y, van Waerbeke L. 2002. *Astron. Astrophys.* 389:L28
 Bernardeau F, Valageas P. 2000. *Astron. Astrophys.* 364:1
 Bernardeau F, van Waerbeke L, Mellier Y. 1997. *Astron. Astrophys.* 322:1
 Bernardeau F, van Waerbeke L, Mellier Y. 2003. *Astron. Astrophys.* 397:405
 Berstein GM, Jarvis M. 2001. astro-ph/0107431
 Blandford RD, Saust AB, Brainerd TG, Villumsen JV. 1991. *MNRAS* 241:600
 Bonnet H, Mellier Y. 1995. *Astron. Astrophys.* 303:331
 Borgani S, Rosati P, Tozzi P, Stanford SA, Eisenhardt PR, et al. 2001. *Ap. J.* 561:13
 Boulade O, Charlot X, Abbon P, Aune S, Borgeaud P. et al. 2000. *Proc. SPIE* 4008:657 *Megacam Home Page*.
<http://www-dapnia.cea.fr/Phys/Sap/Activites/Projets/Megacam/page.shtml>
 Brown M, Taylor AN, Hambly N, Dye S. 2000. astro-ph/0009499
 Brown M, Taylor AN, Bacon, D.J., Gray, M.E., Dye S., Meisenheimer, K., Wolf, C. 2003. *MNRAS* 341:100
 Catalan P, Kamionkowski M, Blandford R. 2001. *MNRAS* 320:7
 Chang T-C, Refregier A. 2002. *Ap. J.* 570:447
 Contaldi, C, Hoekstra, H., Lewis, A. 2003. submitted to *Phys. Rev. Letters*. astro-ph/0302435
 Cooray A. 2002. astro-ph/0206068
 Cooray A, Hu W. 2001a. *Ap. J.* 548:7
 Cooray A, Hu W. 2001b. *Ap. J.* 554:56
 Cooray A, Hu W. 2002. *Ap. J.* 574:19
 Cooray A, Hu W, Miralda-Escudé J. 2000. *Ap. J.* 535:9
 Cooray A, Kesden M. 2002. astro-ph/0204068
 Crittenden R, Natarajan P, Pen U, Theuns, T. 2001a. *Ap. J.* 559:552
 Crittenden R, Natarajan P, Pen U, Theuns T. 2001b. astro-ph/0012336
 Croft RAC, Metzler CA. 2000. *Ap. J.* 545:561
 Eke V, Cole S, Frenk C, Patrick Henry J. 1998. *MNRAS* 298:1145
 Erben T, van Waerbeke L, Bertin E, Mellier Y, Schneider P. 2001. *Astron. Astrophys.* 3667:17
 Fort B, Mellier Y. 1994. *Astron. Astrophys. Rev.* 5:239
 Gray ME, Taylor AN, Meisenheimer K, Dye S, Wolf C, Thommes E. 2002. *Ap. J.* 568:141
 Gunn JE. 1967. *Ap. J.* 150:737
 Hamana T, Colombi S, Mellier Y. 2000. Cosmological Physics with Gravitational Lensing. *Proc. XXth Moriond Astrophys. Meet., Les Arcs, France*, ed. J-P Kneib, Y Mellier, M Mon, J Tran Thanh Van. astro-ph/0009459
 Hamana T, Miyazaki S, Shimasaku K, Furusawa H, Doi M, et al. 2002, submitted to *Ap. J.*, preprint astro-ph/0210450

- Hämmerle H, Miralles JM, Schneider P, Erben T, Fosbury RA. 2002. *Astron. Astrophys.* 385:743
- Heavens AF. 2001. *Intrinsic Galaxy Alignments and Weak Gravitational Lensing*. Yale Worksh. Shapes Galaxies Haloes, May. astro-ph/0109063
- Heavens A, Refregier A, Heymans C. 2000. *MNRAS* 319:649
- Heymans C, Heavens A. 2002. astro-ph/0208220
- Hirata C, Seljak U. 2002. astro-ph/0209489
- Hirata C, Seljak U. 2003. to appear in *MNRAS*. astro-ph/0301054
- Hiroyasu A, et al. 2001. *Subaru Home Page*. <http://www.subaru.naoj.org/>
- Hoekstra H, Franx M, Kuijken K, Squires G. 1998. *Ap. J.* 504:636
- Hoekstra H, Franx M, Kuijken K, Carlberg RG, Yee HKC, et al. 2001. *Ap. J.* 548:5
- Hoekstra H, Yee HKC, Gladders M. 2001. *Ap. J.* 558:11
- Hoekstra H, Yee HKC, Gladders M. 2002a. *Ap. J.* 577:595
- Hoekstra H, Yee HKC, Gladders M. 2002b. astro-ph/0205205
- Hoekstra H, Yee HKC, Gladders M, Felipe Barrientos L, Hall PB, Infante L. 2002a. *Ap. J.* 572:55
- Hoekstra H, van Waerbeke L, Gladders MD, Mellier Y, Yee HKC. 2002b. *Ap. J.* 577:604
- Hu W. 1999. *Ap. J.* 522L:21
- Hu W. 2000. *Phys. Rev. D* 63:3504
- Hu W. 2001. astro-ph/010890
- Hu W. 2002. astro-ph/0208093
- Hu W, Keeton CR. 2002. astro-ph/0205412
- Hu W, Tegmark M. 1999. *Ap. J.* 514L:65
- Hu W, White M. 2000. *Ap. J.* 554:67
- Hui L. 1999. *Ap. J.* 519:9
- Huterer D. 2001. astro-ph/0106399
- Jain B, Seljak U. 1997. *Ap. J.* 484:560.
- Jain B, Seljak U, White S. 2000. *Ap. J.* 530:547
- Jain B, van Waerbeke L. 2000. *Ap. J.* 530:L1
- Jaroszynski M, Park C, Paczyński B, Gott JR. 1990. *Ap. J.* 365:22
- Jarvis, M., Bernstein, G.M., Fisher, P., Smith, D., Jain, B., Tyson, J.A., Wittman, D. 2002, *Ap. J.* 125:1014
- Jing YP. 2002. *MNRAS* 335:L89
- Kaiser N. 1992. *Ap. J.* 388:272.
- Kaiser N. 1998. *Ap. J.* 498:26.
- Kaiser N. 1999. *Weak Lensing by Galaxy Clusters*. Boston Lensing Meet. astro-ph/9912569
- Kaiser N. 2000. *Ap. J.* 537:555
- Kaiser N, Squires G, Broadhurst T. 1995. *Ap. J.* 449:460
- Kaiser N, Tonry JL, Luppino GA. 2000. *PASP* 112:768. *Pan-STARRS homepage* <http://pan-starrs.ifa.hawaii.edu/>
- Kaiser N, Wilson G, Luppino GA. 2000. astro-ph/0003338
- Kaiser N, Wilson G, Luppino GA, Dahle H. 1999. astro-ph/99077229
- Kaiser N, Wilson G, Luppino G, Kofman L, Gioia I, et al. 1998. astro-ph/9809268
- Kamionkoski M, Babul A, Cress CM, Refregier A. 1997. *MNRAS* 301:1064. astro-ph/9712030
- King L, Schneider P. 2002a. astro-ph/0208256
- King L, Schneider P. 2002b. astro-ph/0209474
- Kristian J, Sachs RK. 1966. *Ap. J.* 143:379
- Kristian J. 1967. *Ap. J.* 147:864
- Kuijken K. 1999. *Astron. Astrophys.* 352:355
- Kuijken K, Bender R, Cappellaro E, Musciello B, Baruffolo A et al. 2002. *ESO Messenger* 110: 15; VST homepage <http://www.na.astro.it/vst/>
- Lee MH, Paczyński B. 1990. *Ap. J.* 357:32
- Lee J, Pen U. 2001. *Ap. J.* 532:5
- Luppino GA, Kaiser N. 1997. *Ap. J.* 475:20
- Ma C-P. 1998. *Ap. J.* 508:5
- Mackey J, White M, Kamionkowski M. 2001. astro-ph/0106364
- Massey R., Rhodes J., Refregier A., Albert J., Bacon D. et al. 2003. astro-ph/0304418
- Maoli R, van Waerbeke L, Mellier Y, Schneider P, Jain B, et al. 2001. *Astron. Astrophys.*, 368:766
- Mellier Y. 1999. *Annu. Rev. Astron. Astrophys.* 37:127

- Mellier Y, van Waerbeke L, Bertin E, Tereno I, Bernardeau F. 2002. astro-ph/0210091
- Mellier Y, van Waerbeke L, Maoli R, Schneider P, Jain B, et al. 2001. Cosmic shear surveys. *Deep Fields, Proc. Eur. South. Obs., Oct., Garching*, Ger. astro-ph/0101130
- Mellier Y, van Waerbeke L, Radovich M, Bertin E, Dantel-Fort M. 2000. *ESO Proceedings, Mining the Sky, Garching, July 2000*, A.J. Banday et al eds. astro-ph/0012059. CFHTLS homepage <http://cdsweb.u-strasbg.fr:2001/Science/CFHLS/>
- Mould J, Blandford R, Villumsen J, Brainerd T, Smail I. 1994. *MNRAS* 271:31
- Miyazaki S, Hamana T, Shimasaku K, Furusawa H, Doi M, et al. 2002. *Ap. J.* 580:97
- Munshi D, Coles P. 2000. astro-ph/0003354
- Munshi D, Coles P. 2002. astro-ph/0003481
- Munshi D, Jain B. 2000. *MNRAS* 318:109
- Munshi D, Jain B. 2001. *MNRAS* 322:107
- Munshi D, Wang Y. 2002. astro-ph/0206483
- Narayan R, Bartelmann M. 1999. In *Formation of Structure in the Universe*, ed. A Dekel, JP Ostriker, p. 360. astro-ph/9606001
- Padmanabhan N, Seljak U, Pen UL. 2002. *New Astronomy* 8:581
- Peacock J, Dodds SJ. 1997. *MNRAS* 280:L19
- Pen U, Lee J, Seljak U. 2000. *Ap. J.* 543:L107
- Pen U, van Waerbeke L, Mellier Y. 2001. astro-ph/0109182
- Perlmutter, et al. 2003. *SNAP Home Page*. <http://snap.lbl.gov>
- Pierpaoli E, Scott D, White M. 2001. *MNRAS* 325:77
- Pierpaoli E, Scott D, White M. 2002. submitted to *MNRAS*. astro-ph/0210567
- Premadi P, Martel H, Matzner R, Futamase T. 2001. *Ap. J. Suppl.* 135:7
- Refregier A. 2003. *MNRAS* 338:35
- Refregier A, Bacon DJ. 2003. *MNRAS* 338:48
- Refregier A, Rhodes J, Groth E. 2002. *Ap. J.* 572:L131
- Refregier A, Brown ST, Kamionkowski M, Helfand DJ, Cress CM, et al. 1998. Wide Field Surveys in Cosmology. *Proc. XIVth IAP Meet.*, ed. Y Mellier, S Colombi. Paris. astro-ph/9810025
- Refregier A, Massey M, Rhodes J, Ellis R, Albert J, et al. 2003. astro-ph/0304419
- Reiprich TH, Böhringer H. 2001. astro-ph/0111285
- Rhodes J, Refregier A, Groth E. 2000. *Ap. J.* 536:79
- Rhodes J, Refregier A, Groth E. 2001. *Ap. J.* 552:L85
- Rhodes J., Refregier A., Massey R., Albert, J., Bacon D., et al. 2003, astro-ph/0304417
- Schneider P. 1995. *Proc. Laredo Adv. Summer Sch.*, Sept. astro-ph/9512047
- Schneider P. 1998. *Ap. J.* 498:43
- Schneider P. 1999. *Proc. Perspec. Radio Astron., April, Amsterdam*. astro-ph/9907146
- Schneider P, Lombardi M. 2002. astro-ph/0207454
- Schneider P, van Waerbeke L, Jain B, Kruse G. 1998a. *MNRAS* 296:873
- Schneider P, van Waerbeke L, Kilbinger M, Mellier Y. 2002. *Astron. Astrophys* 396:1
- Schneider P, Weiss A. 1988. *Ap. J.* 327:526
- Schneider P, van Waerbeke L, Mellier Y, Jain B, Seitz S, Fort B. 1998b. *Astron. Astrophys.* 333:767
- Seljak U. 1996. *Ap. J.* 463:1
- Seljak U. 2001. astro-ph/0111362
- Seljak U, Zaldarriaga M. 1999. *Phys. Rev. D* 60:43504
- Smith RE, Peacock JA, Jenkins A, White SDM, Frenk CS, et al. 2003. *MNRAS* 341:1311
- Spergel, D., Verde, L., Peiris, H.V., Komatsu, E., Nolte, M.R., et al. 2003, submitted to *Ap. J.*. astro-ph/0302209
- Stebbins A. 1996. astro-ph/9609149
- Stebbins A, McKay T, Frieman JA. 1995. *Proc. IAU Symposium 173*. astro-ph/9510012
- Takada M, Jain B. 2002. astro-ph/0205055
- Taylor A. 2001. astro-ph/0111605
- Taylor A, Watts P. 2000. astro-ph/0010014
- Taylor A, et al. 2003. in preparation *VISTA Home Page*. <http://www.vista.ac.uk>
- Tyson JA, Wittman D, Hennawi JF, Spergel DN. 2002a. *Proc. 5th Int. UCLA Symp. Sources Detect. Dark Matter*, Feb., Marina del Rey, ed. D Cline. astro-ph/0209632
- Tyson JA, & the LSST collaboration 2002b. *Proc. SPIE Int.Soc.Opt.Eng.* 4836, 10-20. astro-ph/0302102. *LSST Home Page* <http://lsst.org>
- Uzan J-P, Bernardeau F. 2001. *Phys. Rev. D* 64:083004

- Valageas P. 2000. *Astron. Astrophys.* 356:771
- Valdes F, Jarvis JF, Tyson JA. 1983. *Ap. J.* 271:431
- van Waerbeke L. 1998. *Astron. Astrophys.* 334:1
- van Waerbeke L, Bernardeau F, Mellier Y. 1999. *Astron. Astrophys.* 342:15
- van Waerbeke L, Mellier Y., Erben T., Cuillandre JC, Bernardeau F, et al. 2000. *Astron. Astrophys.* 358:30
- van Waerbeke L, Mellier Y., Radovich M., Bertin E., Dantel-Fort M. et al. 2001a. *Astron. Astrophys.* 374:757
- van Waerbeke L, Hamana T, Scoccimarro R, Colombi S, Bernardeau F. 2001b. *MNRAS* 322:918
- van Waerbeke L, Mellier Y, Pelló R, Pen U-L, McCracken HJ, Jain B. 2002. *Astron. Astrophys.* 393:369
- Viana P, Liddle A. 1999. *MNRAS* 303:535
- Viana P, Nichol RC, Liddle A. 2001. astro-ph/0111394
- Villumsen J. 1995. astro-ph/9507007
- Villumsen J. 1996. *MNRAS* 281:369
- van Waerbeke L, Mellier Y, Tereno I. 2002. astro-ph/0206245
- Wambsganss J, Cen R, Ostriker JP. 1998. *Ap. J.* 494:29
- Weinberg NN, Kamionkowski M. 2002. astro-ph/0210134
- White M, Hu W. 2000. *Ap. J.* 537:1
- Wilson G, Kaiser N, Luppino GA. 2001. *Ap. J.* 556:601
- Wittman DM, Tyson J, Kirkman D, Dell'Antonio I, Bernstein G. 2000. *Nature* 405:143
- Wittman DM. 2002. *Dark Matter and Gravitational Lensing, LNP Top. Vol.*, ed. F Courbin, D Minniti. Springer-Verlag. astro-ph/0208063
- Wittman DM, Tyson JA, Dell'Antonio IP, Becker AC, Margoniner VE, et al. 2002. *Proc. SPIE* 4836 v.2. astro-ph/0210118. *Deep Lens Survey web page* <http://dls.bell-labs.com/>
- Zaldarriaga M, Scoccimarro R. 2002. astro-ph/0208075
- Zaldarriaga M, Seljak U. 1998. astro-ph/9810257